Comparative EIS study of the adsorption and electro-oxidation of thiourea and tetramethylthiourea on gold electrodes

A. E. Bolzán & L. M. Gassa

Journal of Applied Electrochemistry

ISSN 0021-891X
Volume 44
Number 2

J Appl Electrochem (2014) 44:279-292
DOI 10.1007/s10800-013-0621-7

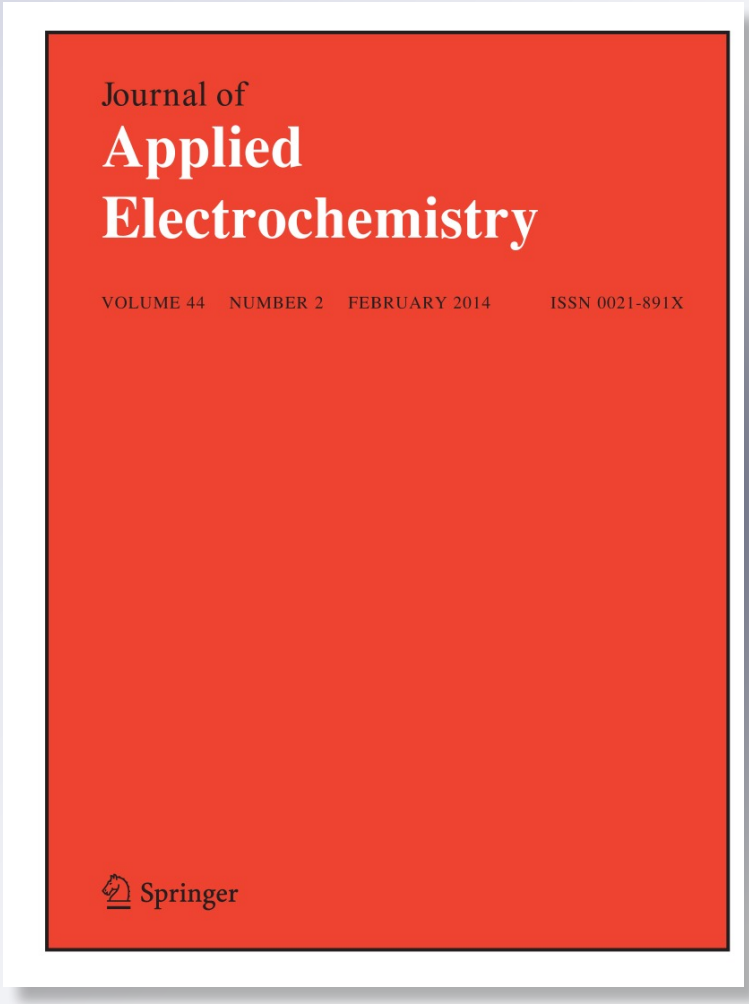

Springer

J Appl Electrochem (2014) 44:279–292
DOI 10.1007/s10800-013-0621-7

RESEARCH ARTICLE

Comparative EIS study of the adsorption and electro-oxidation of thiourea and tetramethylthiourea on gold electrodes

A. E. Bolzán · L. M. Gassa

Received: 7 June 2013 / Accepted: 20 August 2013 / Published online: 31 August 2013

Abstract A comparative study of the electrochemical behaviour of thiourea (TU) and tetramethylthiourea (TMTU) on gold in sulphuric acid was performed using a gold rotating disc electrode. The electrochemical impedance spectra are interpreted through an equivalent circuit involving the electrolyte resistance, a constant phase element for the capacity double layer, a charge transfer resistance and, depending on the electrode potential, a second parallel impedance element whose interpretation depends on the potential region considered. Thus, for both thioureas, the Nyquist plots for $E < -0.6$ V (vs. MSE) exhibit a single capacitive time constant related to the adsorption of the molecule on the electrode surface. As E increases, the Nyquist plots exhibit a new time constant assigned to the formation of a soluble complex species. This time constant appears in the potential region also related to the electro-oxidation of the thioureas to the corresponding formamidinium disulphide. This means that these processes are coupled and, therefore, only one time constant can be observed. An inductive loop at low frequencies is associated with the pitting of the gold electrode for $E \geq -0.20$ V, in agreement with SEM micrographs. The value of the corresponding charge transfer resistance decreases markedly with the electrode potential, indicating the increase in the rate of the electrochemical processes. Electrodissolution of gold results more importantly in the presence of TMTU. At potential values associated with the formation of the anodic oxide layer on gold, a negative resistance is recorded, indicating the passivation of the electrode surface. Eventually, at $E > 0.6$ V, the electrode surface passivation disappears and the Nyquist plots exhibit two strongly overlapped capacitive constants assigned to the oxide film growth at the monolayer level and the second electro-oxidation process of thioureas, the latter resulting in the formation of carbon dioxide and sulphate ions according to FTIRRAS data.

Keywords Gold · Thiourea · Tetramethylthiourea · EIS · Electro-oxidation · Electrodissolution

1 Introduction

The extraction of gold from its host mineral is based on the use of lixiviants such as cyanide (in alkaline medium), chlorine and thiourea (in acidic medium). Cyanide is currently used in most commercial operations because of its low cost and process simplicity. However, it is disadvantaged by slow dissolution kinetics, poor selectivity and severe environmental constraints, related to tailings disposal, water quality and the environmental impacts [1]. These factors have emphasised the need for alternative lixiviants, among them are those involving S-containing molecules, such as thiosulphate [2], thiocyanate [3] and thiourea [4] solutions.

Thiourea (TU) has been proposed as a cyanide alternative for the recovery of gold and silver from minerals in hydrometallurgy [5–11], particularly at high concentrations and in the presence of an appropriate oxidant such as ferric sulphate [9]. For the case of gold and TU several complexes such as $[Au(TU)_2]Br$ [12], $[Au(TU)_2]Cl$ [13] and $[Au(TU)_2]_2SO_4$ [13], involving the $[Au(TU)_2]^+$ ion, have been studied by X-ray diffractometry. However, in the case

A. E. Bolzán (✉) · L. M. Gassa
Instituto de Investigaciones Fisicoquímicas Teóricas y Aplicadas - INIFTA, UNLP, CONICET, Sucursal 4, Casilla de Correo 16, 1900 La Plata, Argentina
e-mail: aebolzan@inifta.unlp.edu.ar

of TMTU, only some evidence of their formation has been reported [14, 15], as their synthesis seems to be hard to obtain.

It has been reported that gold is dissolved more efficiently by TU in acidic solution than in alkaline solution. TU is unstable above pH = 4.3, and degradation of the TU also takes place due to oxidation. TU is oxidised to formamidine disulphide, which is an active oxidant for gold dissolution. Formamidine disulphide is also oxidised to a number of intermediate species where elemental sulphur is the final product. The formation of elemental sulphur causes passivation of precious metals and the dissolution will tend to cease [16, 17]. Spectrochemical investigations of gold leaching in TU solutions indicated that TU is adsorbed at the electrode surface even at potentials related to the hydrogen evolution reaction and an amorphous sulphide/polysulphide phase is formed in the potential region related to TU oxidation [18].

The electro-oxidation of TU on gold in acid solutions takes place in the potential range of both gold immunity and gold corrosion [5], although the relative contributions of TU and gold electro-oxidation reactions depend on both the TU concentration and the range of applied potential. However, although the overall electro-oxidation process has been studied by a number of conventional electrochemical techniques [4, 5, 9, 19], the available kinetic data and conclusions on the reaction mechanism are not thoroughly consistent. In acid, gold electrodissolution proceeds with 100 % efficiency for $E < 0.3$ V (SHE), while for $E > 0.3$ V the reaction is accompanied by TU electro-oxidation to formamidine disulphide (FDS) and by-products, decreasing the efficiency of the reaction [19]. According to in situ FTIRRAS measurements, the electro-oxidation of TU on gold produces soluble $[Au(TU)_2]_2SO_4$ and FDS at potentials below 1.2 V (SHE) and carbon dioxide, sulphate ions and CN-containing species above this potential [20]. Combined FTIRRAS and DEMS studies also showed the formation of nitrogen as oxidation product and the possible formation of hydrogen sulphide as a reduction species [21].

TMTU exhibits some similarities with TU, such as the formation of a formamidinium disulphide (tetramethylformamidinium disulphide, $TMFDS^{2+}$), either under electrochemical [15] or homogeneous chemical [22–24] oxidation conditions. Scanning tunnelling microscopy (STM) studies on gold single-crystal electrodes also showed that TMTU also produces electrochemical etching of the gold surface [25, 26]. According to capacitance measurements [25] the adsorption of TMTU on gold takes place in the range −0.25 to 0.8 V versus the standard hydrogen electrode, (SHE) and its desorption occurs at ca. 0.85 V (SHE). A substantial adsorption of TMTU has been inferred from the low and almost-constant capacity of 10–13 μF cm^{-2} measured in the range −0.25 to 0.8 V (SHE). Seemingly, the structure of the TMTU adsorbate depends on the nature of the metal electrode. Thus, for Au (1 1 1) the surface excess decreases to 2.1×10^{-10} mol cm^{-2} and the TMTU molecules lie almost flat on the gold surface with a slight tilt arising from the local spatial requirements of methyl groups [26]. The adsorption of TMTU on polycrystalline gold in both acid and base has also been investigated by SNIFTIRS [27]. From *p*- and *s*-polarised light spectra it has been concluded that the TMTU molecule adsorbs with the NCSN plane parallel to the electrode surface.

At sufficiently positive potentials, gold electrodissolution takes place via the formation of a soluble gold–TMTU complex [15, 25, 27], although neither IR nor X-ray diffraction data for this complex species have been reported. Gold single-crystal data show that surface etching starts at step edges and eventually produces monoatomic steps with a preferred orientation [14]. The resulting soluble TMTU–gold complex species can be reduced at sufficiently negative potentials yielding gold islands through a nucleation and growth mechanism.

The comparison of chemical and electrochemical data of TU and TMTU on gold indicates that the feasibility of using either TU or TMTU for metal lixiviation is closely connected to the formation of soluble complex species between the metal and the organic molecule and consequently to the behaviour of these molecules on the gold surface, i.e. the proper characteristics of the adsorption and electro-oxidation processes. In this respect, the electrochemical behaviour of TU has been more extensively studied than TMTU. The aim of this work is to advance in the knowledge of the electrochemical behaviour of TMTU on gold in comparison with that of thiourea. For this purpose, electrochemical impedance spectroscopy (EIS) was employed to study the steady-state behaviour of both TU and TMTU covering the potential range related to their electroadsorption and electro-oxidation on gold, complemented with steady-state polarisation curves and SEM and FTIRRAS measurements. As it has been already shown that gold dissolution and TUs electro-oxidation are electrochemical processes under diffusion control [15, 28, 29], a gold disc electrode rotating at 2,000 rpm was used to minimize mass transfer effects during the electrochemical measurements. The analysis of the impedance spectra provides valuable information about the behaviour of TU and TMTU on the gold electrode in the potential range related to the thermodynamic stability of water.

2 Experimental

The EIS experiments were made using a conventional glass three-electrode cell utilising a gold rotating disc electrode

(geometric area 0.125 cm^{-2}) as working electrode. This electrode was polished mechanically using alumina–water suspension and washed thoroughly with water before each experiment. The counter electrode was a large platinum sheet (2 cm^2 apparent area) and the reference electrode was a mercurous sulphate electrode (MSE, saturated K_2SO_4 solution). The working solutions were prepared from TU (Fluka, puriss. p.a.) or TMTU (Fluka, p.a.) and sulphuric acid (97 % Merck, p.a.) using Milli-Q* water. Solutions were kept under nitrogen saturation before and during the experiment.

Electrochemical impedance measurements were carried out using a Zahner IM6d potentiostat with frequency analyser. The experiments were performed applying a sine waveform perturbation with amplitude 5×10^{-3} V to the electrode potential, while scanning the modulus of impedance and the phase shift in the frequency range $10^{-3} \leq f \leq 10^5$ Hz. The applied potential was increased in 0.050 V steps from −0.80 to 1.0 V. Complementary runs were made using a Radiometer Voltalab 10 potentiostat.

EIS experiments were complemented with FTIRRAS data obtained using a flow cell to establish the formation of TU and TMTU adsorbates on gold. For this purpose, an electrochemical cell consisted of a conventional three-electrode design [30] with a fluorite 60° prism at the bottom of the cell. A polycrystalline gold disc (1.2 cm dia.) was used as the working electrode. Before each run, this electrode was polished to mirror grade with 0.3-μm-grid alumina and rinsed with Milli-Q* water. A platinum sheet and a reversible hydrogen electrode in the working solution were used as counter and reference electrode, respectively. The cell was filled with ca. 7 ml of aqueous either 0.1 M TMTU or 0.1 M TU in 0.1 M $HClO_4$, and the gold electrode was held at 0.05 V for 300 s. Then, the working electrode was pulled up few millimetres at constant potential to allow the full replacement of the solution in the cell by flowing 200 ml of plain aqueous 0.1 M $HClO_4$. Subsequently, the working electrode was put once again in contact with the prismatic window to record a reference spectrum at $E_{ref} = 0.05$ V. Afterwards, E was stepped to either 1.2, 1.5 or 1.6 V to electro-oxidise strongly bound residues and 1000 interferograms using p-polarised light were collected. The working solutions were prepared from perchloric acid (70 % Alfa Aesar, p.a.), TU or TMTU (Fluka, p.a) and Milli-Q* water. FTIRRAS measurements were performed using a Nicolet Nexus 670 FTIR spectrometer coupled to a Wenking 72L potentiostat. Normalised reflectance spectra were calculated as R/R_0 ratio, where R is the value of the reflectance at the sampling potential E_s and R_0 is the reflectance measured at the reference potential, $E_{ref} = 0.05$ V. Positive and negative absorption bands represent the loss and gain of species at E_s as compared to E_{ref}, respectively.

Micrographs of gold electrodes, to observe possible etching on the surface by the action of the TUs, were obtained with XL30 FEG Philips SEM equipment.

All the experiments were made at 298 K and potentials in the text are given in the MSE scale (0.65 V vs. NHE).

3 Results and discussion

3.1 Steady-state polarisation curves

Steady-state polarisation curves for TU and TMTU on the gold disc rotating at 2,000 rpm show regions with different current/potential functionalities, as expected for a change in the kinetics of the process at different potentials. Thus, for 1 mM concentration, the polarisation curve for TU exhibits a practically null current plateau from –0.8 V up to about –0.4 V (Fig. 1a, full trace) followed by a rapid current increase that results in the appearance of a current peak at ca. 0.5 V. This current peak exhibits two shoulders, at ca. 0.3 and ca. 0.7 V, i.e. during the ascending and descending side of the peak, respectively. At 0.8 V, the polarisation curve shows a minimum from which the current rises again.

The polarisation curve corresponding to TMTU (Fig. 1a, dashed trace) shows a small cathodic rather limiting current between –0.8 and –0.4 V. Then, it exhibits an almost null current plateau from –0.4 to –0.2 V and afterwards

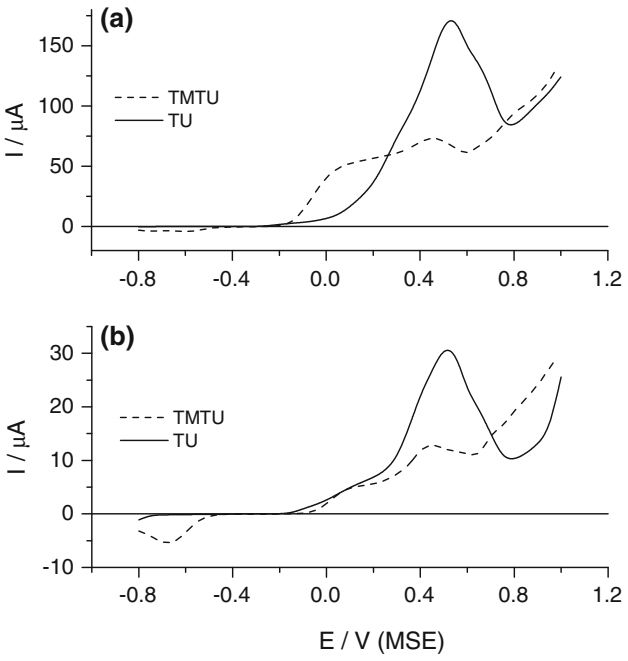

Fig. 1 Steady-state polarisation curves for TU and TMTU on a rotating gold disc electrode in 0.5 M sulphuric acid at two different concentrations: **a** 1 mM, **b** 0.1 mM. ω = 2,000 rpm. T = 298 K

increases from ca. –0.3 V upwards, exhibiting two overlapped broad anodic current peaks at ca. 0.0 and ca. 0.45 V. Then, the current decreases as the potential increases towards 0.6 V, a potential value from which the current starts to increase once again.

When the TUs concentrations are decreased to 0.1 mM, no major changes are observed in the shape of the polarisation curves, irrespective of the TUs, although the current decreases markedly but not directly proportional to the TUs concentrations. The TU polarisation curve shows a current hump at ca. 0.1 V followed by an anodic peak at ca. 0.5 V, a current decrease from 0.5 to 0.8 V and a subsequent current increase from 0.8 V upwards. Thus, in the potential range related to anodic processes, the major difference observed when the TU concentration is decreased is the increase in the anodic current contribution in the 0.0–0.02 V.

In the case of TMTU (Fig. 1b, dashed trace), the polarisation curve shows a slight irreversibility in the current response with respect to 1 mM TMTU (Fig. 1a, dashed trace) and also a slight decrease in the limiting current recorded between 0.1 and 0.25 V.

The anodic electrochemical response of TU and TMTU on gold suggests that seemingly similar processes take place in the same potential region, although as the concentration is increased, the oxidation process begins at lower potentials for TMTU than for TU. Then, from the comparison of the steady-state polarisation curves, one can roughly distinguish three main potential regions. The first one is related to the absence of anodic processes between –0.8 and –0.4 V, where TMTU exhibits a particular cathodic contribution. This region can be related to the adsorption of TUs and possible interaction of hydrogen atoms that results in the formation of S-containing species. The adsorption of TU at the surface of gold electrodes has been observed by SERS measurements, which also suggested the formation of covalent bond between TU and Au [18], and voltammetric runs [29]. The formation of strong adsorbed TMTU species on gold electrodes has been reported from FTIRRAS measurements [15]. Furthermore, FTIRRAS spectra obtained from gold in TMTU acid solutions showed the appearance of bands in the –0.6 to –0.8 V range corresponding to the formation of SH species [15]. This can explain the appearance of a cathodic current in the polarisation curves in the same potential range (Fig. 1a,b, dashed traces). DEMS data also showed the presence of a mass signal corresponding to the formation of H_2S at about –0.65 V [21].

The second potential region is related to the appearance of anodic currents, i.e. between –0.2 and 0.8 V, before the current minimum observed at 0.6 V, for TMTU, and 0.8 V, for TU (Fig. 1a, b). Previous work [15, 21, 29, 31, 32] indicates that this potential region corresponds to two competitive electro-oxidation processes, namely, the electrodissolution of gold forming a soluble complex species and the formation of a formamidinium disulphide from either TU or TMTU molecules. Rotating ring [15, 28] and ring disc [29] data clearly showed that in this potential range the electrochemical processes are related to the formation of soluble products. The voltammetric similarity observed with TU data obtained with Pt electrodes [33] suggested that the main electro-oxidation processes were related to the electro-oxidation of TUs to their corresponding disulphide species in a two-electron process. However, EQCM data for both TU [28, 31] and TMTU [34] suggested that the main contribution was related to the electrodissolution of gold. Furthermore, FTIRRAS data showed the concomitant appearance of bands corresponding to the formation of the gold-soluble species and the formamidinium disulphide for both TU [32] and TMTU [15]. Seemingly, the electro-oxidation of TMTU predominates for $E > -0.1V$ (0.55 V vs. NHE) whereas the formation of soluble gold species predominates at lower potentials [15]. Similar results were reported for TU, i.e. bands related to the appearance of gold complex in solution appear slightly before that related to the formation of the disulphide, but afterwards these processes occur concomitantly. For the case of TU, a quantitative analysis of the IR bands indicated that the band associated with the presence of the soluble complex prevailed over the one corresponding to the formation of FDS, i.e. the dissolution of gold resulted more importantly in this potential region [21].

The third potential region is related to the rather linear increase of the anodic current. This region also corresponds to the formation of the oxide layer on gold in aqueous acid solutions [35]. FTIRRAS and DEMS data [15, 21, 32] indicated that at these potentials the electro-oxidation of either TU or TMTU are further oxidised along with the formation of the oxide gold layer, resulting in the formation of sulphate ions, carbon dioxide, nitrogen and CN-containing species. Besides, SERS data [18] suggest the formation of polysulphide precursor phase on the gold surface and the absence of TU and FDS at the Au surface. This is consistent with the voltammetric data related to the behaviour of strong adsorbed species of both TU and TMTU on gold: in both cases the adsorbates are removed in the 0.8–1.0 V range [15, 29].

3.2 Impedance data

As a first step, the double-layer capacitance of the gold electrode in thiourea-free 0.5 M sulphuric acid solution was determined from impedance measurements performed at E = –0.6 V. From the resulting Nyquist plot (not shown here), a value of 46 μF cm^{-2} was obtained, in good agreement with the literature [27].

3.2.1 EIS of gold electrode in TU-containing solutions

The Nyquist plots resulting from the gold RDE in 1 mM TU + 0.5 M H_2SO_4 show a strong dependence on the applied potential. At sufficiently negative potentials, i.e. –0.8 to –0.75 V, a single capacitive time constant is observed that extends up to 10 mHz (Fig. 2a). For lower frequencies, only a dispersion of impedance values is observed. The response of the system is maintained in shape and real and imaginary values of the impedance for $E < -0.7$ V, and for $E > -0.7$ V an open loop is then observed (Fig. 2b). As E turns more positive the impedance decreases markedly, i.e. about one order of magnitude. From −0.2 up to 0.5 V, the Nyquist plots show the appearance of an inductive loop at low frequencies (Fig. 2c, d), probably associated with the desorption of the TU adsorbate and the electrodissolution of the base metal. At these potentials a yellowish tinge is observed on the platinum counter electrode, indicating that the working electrode is being electrodissolved by the presence of TU.

At E = 0.5 V, one can observed that the inductive loop closes and a second capacitive loop appears from ca. 0.1 Hz downwards (Fig. 3a). This second capacitive loop, however, disappears at E = 0.55 V (Fig. 3b), when the presence of a negative resistance sets in, i.e. the passivation of the electrode surface likely related to the formation of an oxide film at the monolayer level takes place. The appearance of the negative resistance in the Nyquist plots corresponds to the current decrease appearing in the voltammogram at those potentials (Fig. 1a). The passivation stage continues up to E = 0.75 V when two overlapped capacitive constants appear, one for frequencies above 10 Hz and another one from 10 Hz downwards, and the values of the impedance increases about one order of magnitude (Fig. 3c). Eventually, at E = 1.0 V, the capacitive constants overlap completely (Fig. 3d)

When the TU concentration is diminished to 0.1 mM, the Nyquist plots at different potentials exhibit similar features, suggesting that the reaction pathway is not affected by the decrease of TU in solution, although the impedance values are at least one order of magnitude higher than those obtained in 1 mM TU. However, it is interesting to note that the Nyquist plot shows the presence of an inductive contribution already at −0.8 V (Fig. 4a) that disappears at −0.75 V (Fig. 4b). At −0.3 V the Nyquist plot shows an open loop indicating the presence of a very large transfer resistance (Fig. 4c) and at −0.2 V a small inductive contribution is recorded from ca. $f = 0.1$ Hz downwards (Fig. 4d). The inductive loop (Fig. 5a) appears, however, appreciably diminished, as expected for an electrodissolution involving the participation of the soluble TU. Furthermore, the potential values at which the appearance of the different time constants occur are positively shifted with respect to those observed for $c = 1$ mm.

3.2.2 EIS in TMTU-containing solutions

In general, the change from TU to TMTU results in the appearance of some scattering in the Nyquist plots, particularly at low frequencies, a feature that decreases as the

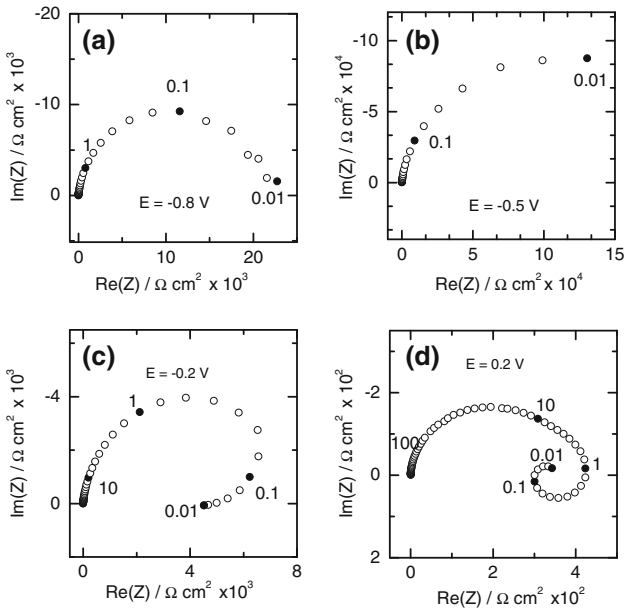

Fig. 2 Nyquist plots corresponding to the gold RDE in 1 mM TU + 0.5 M H_2SO_4 at different potentials. Frequency values (Hz) in the plots correspond to *full dots*. T = 298 K

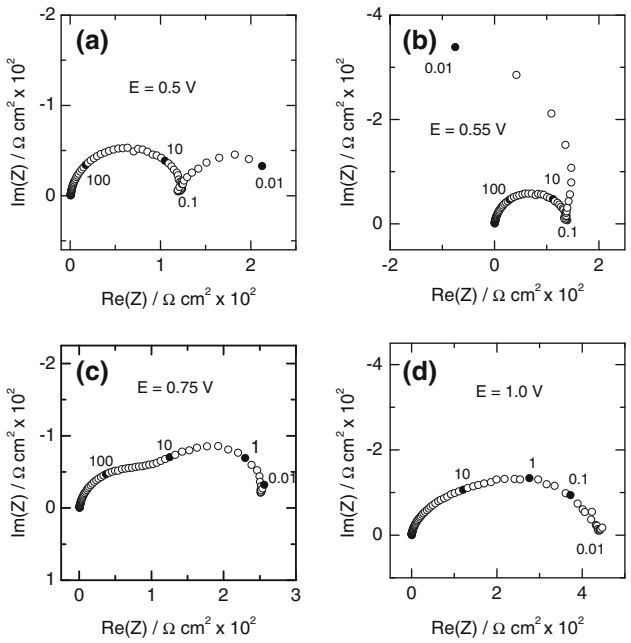

Fig. 3 Nyquist plots corresponding to the gold RDE in 1 mM TU + 0.5 M H_2SO_4 at different potentials. Frequency values (Hz) in the plots correspond to *full dots*

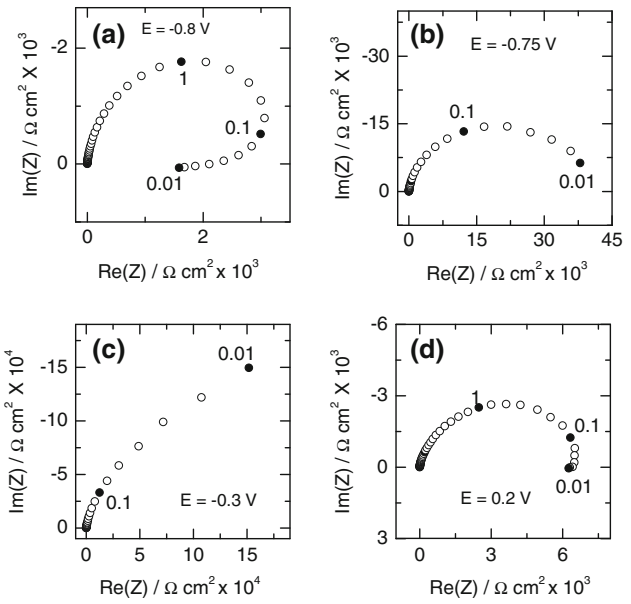

Fig. 4 Nyquist plots corresponding to the gold RDE in 0.1 mM TU + 0.5 M H_2SO_4 at different potentials. Frequency values (Hz) in the plots correspond to *full dots*

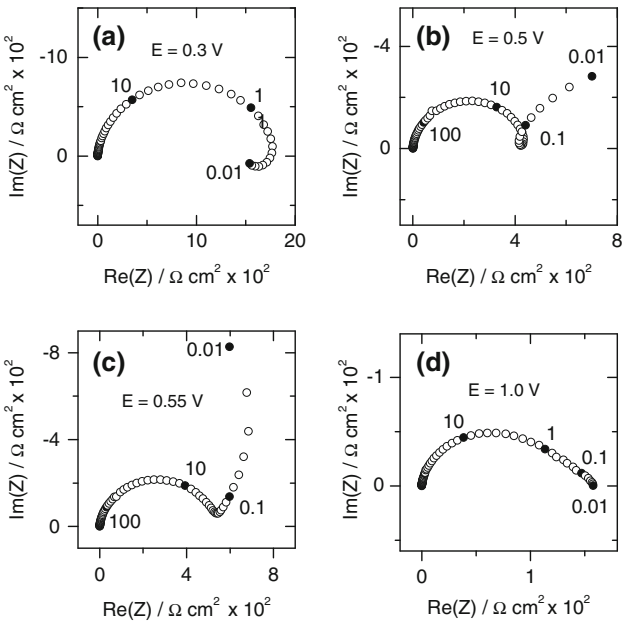

Fig. 5 Nyquist plots corresponding to the gold RDE in 0.1 mM TU + 0.5 M H_2SO_4 at different potentials. Frequency values (Hz) in the plots correspond to *full dots*

TMTU concentration decreases. At variance with TU-containing solutions, the EIS spectra for gold in 1 mM TMTU + 0.5 M H_2SO_4 show the presence of an asymmetric capacitive time constant at −0.8 V (not shown) that agrees with the presence of a small cathodic current in the polarisation curve between −0.5 and −0.8 V (Fig. 1). This suggests that two electrochemical processes take place at this potential. However, as the potential moves towards

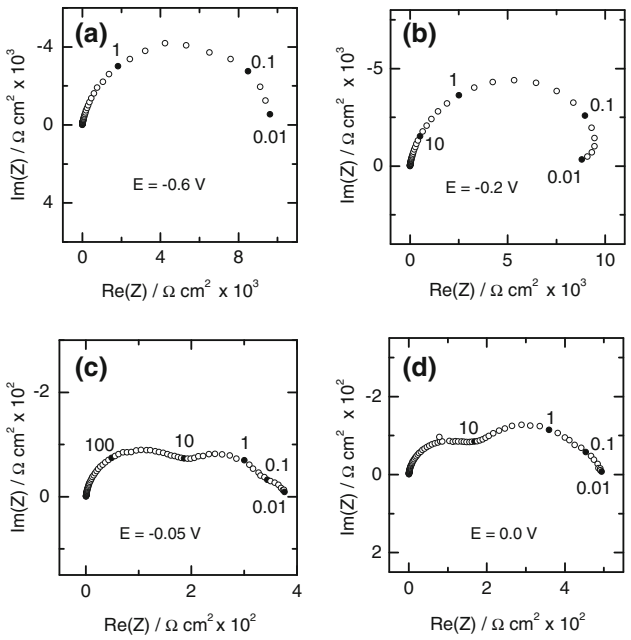

Fig. 6 Nyquist plots corresponding to the gold RDE in 1 mM TMTU + 0.5 M H_2SO_4 at different potentials. Frequency values (Hz) in the plots correspond to *full dots*

–0.6 V (Fig. 6a), the Nyquist plot exhibits a single well-defined semicircle covering the whole range of *f* and, as the potential increases, a delay in the impedance response is also observed, typical of a relaxation process occurring on the electrode surface (Fig. 6b). From −0.10 to 0.15 V, two well-defined semicircles are recorded, one covering frequencies from 100 kHz to 10 Hz and the other from 10 to 0.01 Hz (Fig. 6c). As the potential is made more positive, the impedance of the low-frequency loop increases, whereas that of the high-frequency loop remains constant (Figs. 6c, d and 7a). The presence of two semicircles remain up to ca. 0.2 V, when an incipient inductive loop at low frequencies is once again observed, particularly for E = 0.4 V (Fig. 7 b). At 0.55 V (Fig. 7c) the Nyquist plot shows an inductive loop with a tendency to exhibit a negative resistance at the lowest frequencies, although not as well defined as in the case of TU (Fig. 3b). At 1.0 V the Nyquist plot shows a decrease in the impedance values (Fig. 7d).

When the TMTU concentration is decreased to 0.1 mM, the EIS spectra show significant changes. At $E = -0.8$, the Nyquist plot already shows an inductive contribution in the impedance spectra (Fig. 8a) but as the potential increases this delay disappears and the impedance exhibits a single wide semicircle that starts to open at low frequencies (Fig. 8b). At −0.2 V the spectra clearly show an incomplete capacitive time constant (Fig. 8c). At 0.0 V the Nyquist plot shows once again the appearance of an inductive contribution at low frequencies (Fig. 8d), which continues up to 0.4 V where a small capacitive time

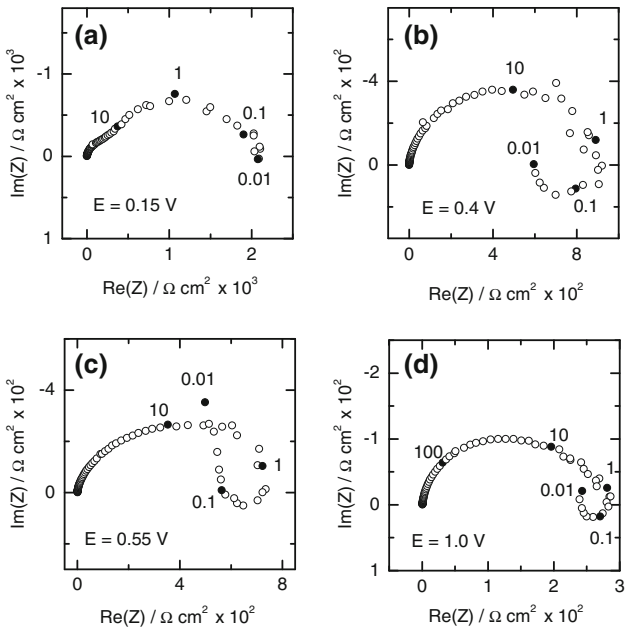

Fig. 7 Nyquist plots corresponding to the gold RDE in 1 mM TMTU + 0.5 M H_2SO_4 at different potentials. Frequency values (Hz) in the plots correspond to *full dots*

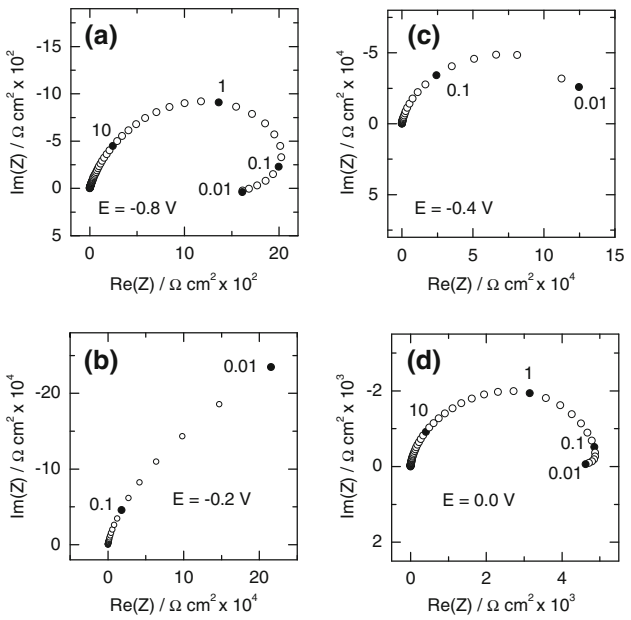

Fig. 8 Nyquist plots corresponding to the gold RDE in 0.1 mM TMTU + 0.5 M H_2SO_4 at different potentials. Frequency values (Hz) in the plots correspond to *full dots*

constant appears below 1 Hz and seemingly decreases the inductive loop (Fig. 9a). As the potential increases, a negative resistance is recorded from 1 Hz downwards, indicating the appearance of a passivation process on the electrode surface (Fig. 9b). It is interesting to note that the contribution of this negative resistance results notably

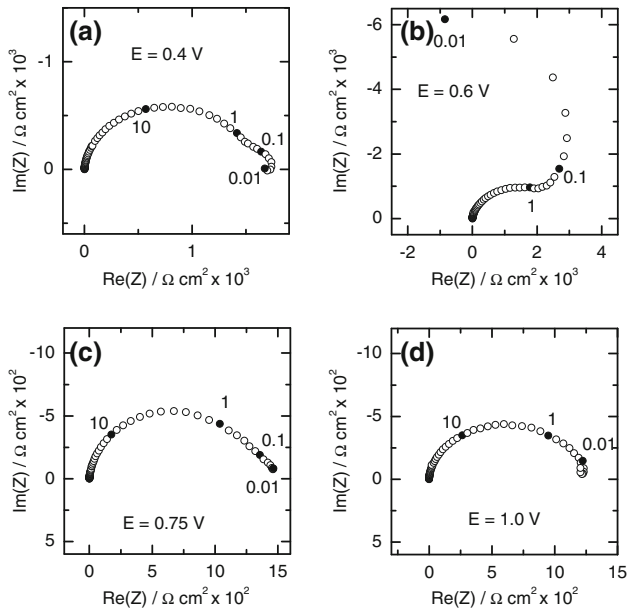

Fig. 9 Nyquist plots corresponding to the gold RDE in 0.1 mM TMTU + 0.5 M H_2SO_4 at different potentials. Frequency values (Hz) in the plots correspond to *full dots*

higher at this lower concentration (compare Figs. 7c, 9b). This passivation process is observed up to ca. 0.7 V where a single broad rather asymmetric time constant is recorded (Fig. 9c) and eventually, from 0.8 V upwards, a small inductive contribution is once again observed at the lowest frequency values (Fig. 9d).

3.3 SEM micrographs

To investigate the possible origin of the inductive loops observed in the Nyquist plots of gold in both TU and TMTU solutions, SEM micrographs were obtained using a gold foil electrode immersed in either 1 mM TU or 1 mM TMTU + 0.5 M H_2SO_4 in the range $0.3 \leq E \leq 0.6$ V for 120 min. The micrographs (Fig. 10) show that, in both cases, the presence of pits on the gold surface was produced by the attack of both TU and TMTU to the electrode surface.

3.4 FTIRRAS data from adsorbed TU and TMTU

The EIS data suggested that both TU and TMTU produce strongly bounded adsorbates on the gold surface at low potentials, which are apparently electro-oxidised at potentials above 0.65 V. FTIRRAS measurements run in a flux cell system allowed to determine the IR bands related to the electro-oxidation products of the adsorbed species. Either TU or TMTU were adsorbed on gold from either 0.1 M TU or 0.1 M TMTU + 0.1 M perchloric acid for 300 s at $E_{ref} = -0.60$ V and subsequently the solution was washed

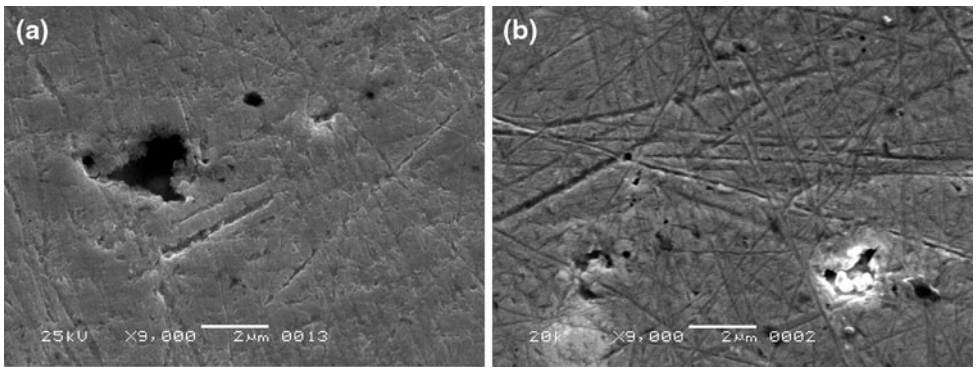

Fig. 10 SEM micrographs of a gold foil anodised at 0.3 V for 120 min in aqueous 1 mM TU + 0.5 M H_2SO_4 (**a**) and 1 mM TMTU + 0.5 M H_2SO_4 (**b**)

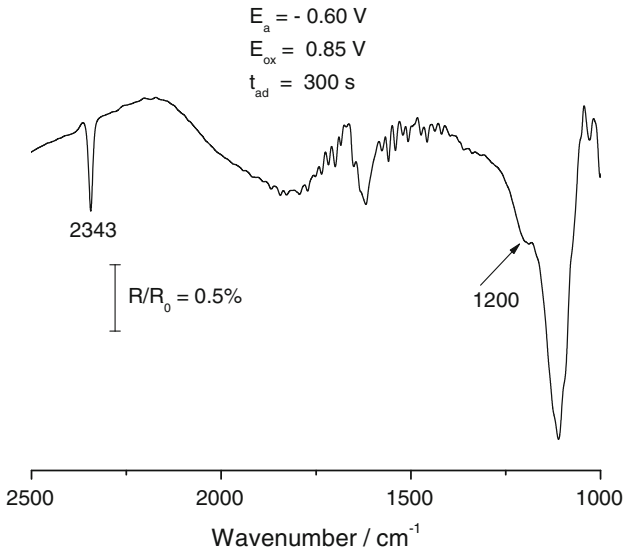

Fig. 11 *p*-Polarised light FTIRRAS spectra for the electro-oxidation of TU adsorbates produced at −0.60 V for 300 s. 0.1 M TU + 0.1 M perchloric acid. $E_{ref} = -0.60$ V

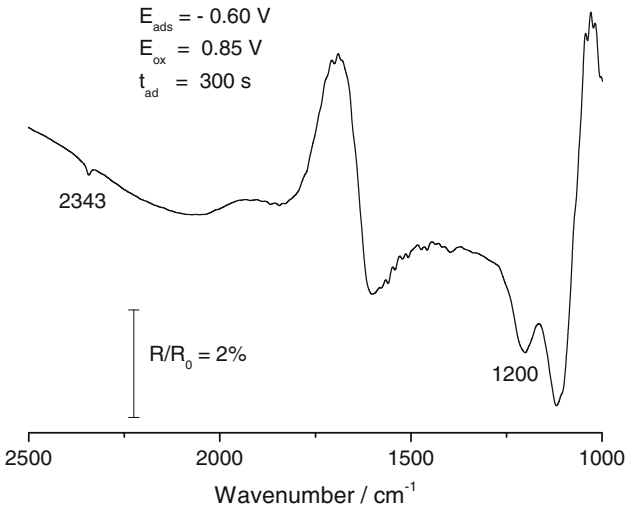

Fig. 12 *p*-Polarised light FTIRRAS spectra for the electro-oxidation of TMTU adsorbates produced at −0.60 V for 300 s. 0.1 M TMTU + 0.1 M perchloric acid. $E_{ref} = -0.60$ V

out by aqueous 0.1 M perchloric acid. Then, a reference spectrum at E_{ref} was recorded before the potential was stepped to 0.85 V. At this potential, the IR spectra show a negative band at 1,100 cm^{-1} corresponding to the perchlorate ions of the base solution, and negative bands at 1,200 and 2,343 cm^{-1} (Figs. 11, 12) corresponding to the apearance of sulphate and carbon dioxide species at the interface. These results show that both thioureas are strongly bounded to the gold surface at negative potentials and the adsorbates are completely electro-oxidised in the potential range related to the formation of the oxide layer on gold [35]. These results are in good agreement with those reported from voltammetric measurements for the electro-oxidation of TU [29] and TMTU adsorbates [15].

4 Discussion

The EIS response resulting from the electrochemical behaviour of TU and TMTU on gold, in the potential region related to the thermodynamic stability of water, can be interpreted in terms of the following general total transfer function:

$$Z_T(j\omega) = R_\Omega + Z(j\omega), \quad (1)$$

where $Z_T(j\omega)$ is the total transfer function; R_Ω is the electrolyte resistance contribution; $\omega = 2\pi f$, f is the frequency and $Z(j\omega)$ is the impedance of the interface that is specific of the electrochemical system. According to the Nyquist spectra described above, the contribution of the interface impedance drastically changes with the electrode potential, as it should be expected for a complex electrochemical system that, as described in previous work, involve several processes, some of them occurring concomitantly in the same potential range. Thus, according to the potential region considered, the electrochemical impedance is interpreted in terms of different equivalent circuits (Fig. 13).

In the case of TU at the lowest potential, i.e. −0.8 V, where only a single semicircle is observed, the interface can be associated with the equivalent circuit 13a, and Z($j\omega$) results

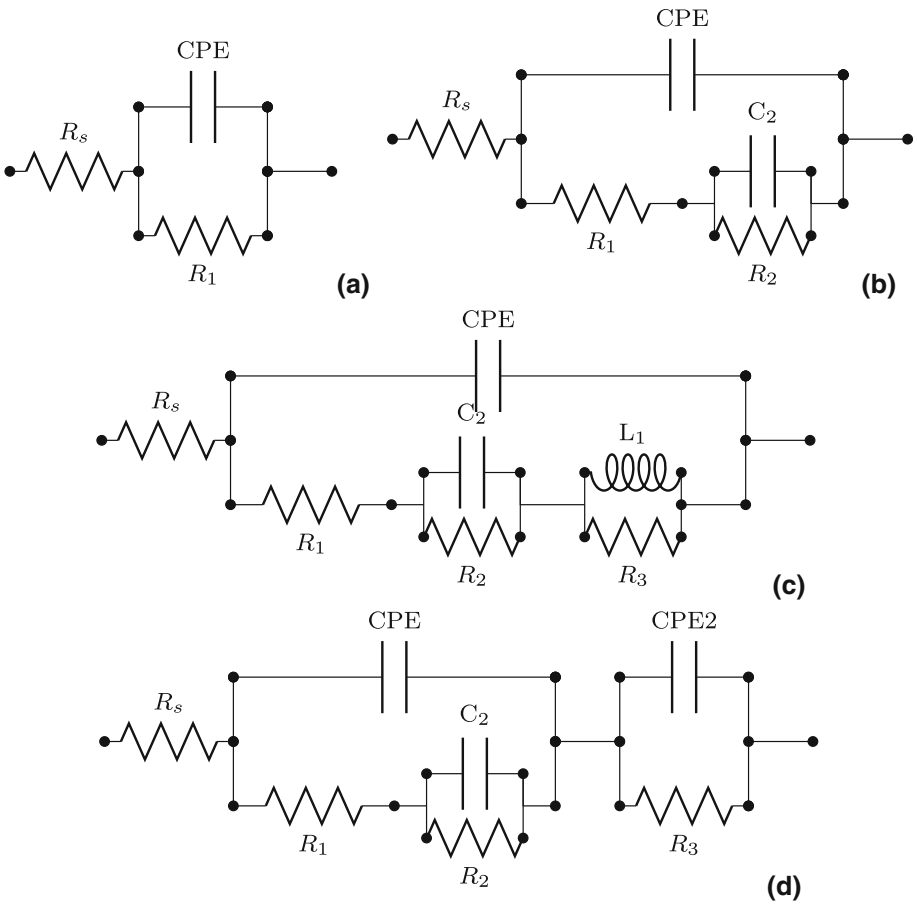

Fig. 13 Equivalent circuits corresponding to the transfer functions given by Eqs. 2 (**a**), 3 (**b**), 4 (**c**) and 5 (**d**)

$$[Z(j\omega)]^{-1} = [Z_{\mathrm{CPE}}]^{-1} + [R_1]^{-1}, \tag{2}$$

where $Z_{\mathrm{CPE}} = [C_{\mathrm{dl}}(j\omega)^{\alpha}]^{-1}$ is the constant phase element; C_{dl} is the double-layer capacitance; the exponent α accounts for the distribution of time constants due to surface inhomogeneities; R_1 is the charge transfer resistance defined as $R_1 = \lim_{\omega\to\infty} \mathrm{Re}[Z]$

However, for both TU and TMTU, as the potential is increased from −0.8 to about 0.25 V, the evolution of the Nyquist plots suggests that the electrochemical interface increases in complexity due to the participation of more than one electrochemical process, a fact that is clearly reflected in the asymmetry of the semicircles and the slow appearance of an inductive contribution at low frequencies. In this case, the electrochemical interface is approached to equivalent circuit 13b and Z(j ω) is given by

$$[Z(j\omega)]^{-1} = [Z_{\mathrm{CPE}}]^{-1} + \left[R_1 + \frac{R_2}{j\omega C_2 R_2 + 1}\right]^{-1}, \tag{3}$$

where R_2 and C_2 are related to the second faradaic pseudo-capacitive contribution of an electrochemical reaction.

From 0.25 and ca. 0.5 V, the Nyquist plot exhibits a net inductive loop with a negative capacitance. Consequently, the interface is approached by the equivalent circuit 13c, whose $Z(j\ \omega)$ is

$$[Z(j\omega)]^{-1} = [Z_{\mathrm{CPE}}]^{-1} + \left[R_1 + \frac{R_2}{j\omega C_2 R_2 + 1} + \frac{j\omega L R_3}{j\omega L + R_3}\right]^{-1}, \tag{4}$$

Afterwards, in a rather limited potential region between 0.55 and 0.65 V thereabouts, the Nyquist plots show the appearance of a negative resistance likely due to the occurrence of an electrochemical reaction that produce, at least, a partial passivation of the electrode surface. This is consistent with the presence of a current minimum in the polarisation curves (Fig. 1). As this new process occurs in series with the former ones, one can include it in the equivalent circuit (circuit 13d), and Z(j ω) results in,

$$[Z(j\omega)]^{-1} = [Z_{\mathrm{CPE}}]^{-1} + \left[R_1 + \frac{R_2}{j\omega C_2 R_2 + 1}\right]^{-1} + [Z_{\mathrm{CPE}_2}]^{-1} + [R_3]^{-1}. \tag{5}$$

The fit of the experimental data (Figs. 2, 3, 4, 5, 6, 7, 8, 9), using conventional non-linear least-square fitting routines, exhibits a good agreement as shown by the

corresponding Bode plots (Figs. 14, 15 and 16). The parameters resulting from the fits are assembled in Table 1.

The good agreement between the experimental and equivalent circuit EIS data, coupled to the SEM and FTIRS additional information, shows that one can explain the electrochemical behaviour of TUs on gold considering three potential regions. Accordingly, depending on the potential region considered, the EIS response involves either 1, 2 or 3 time constants, each one associated with a different electrochemical process. Furthermore, the limits of each potential region depend on whether TU or TMTU are considered.

A first potential region is that related to the adsorption of TUs on gold, i.e. from –0.8 to ca. –0.3 V (Fig. 1). In this case, the Nyquist plots involve a single time constant for the case of TU and two time constants for the case of TMTU (Table 1). This difference is consistent with the characteristics of the corresponding polarisation curves: in the case of TMTU a net cathodic current is recorded in this potential region (Fig. 1). Therefore, for both TUs there is a time constant associated with the adsorption of the molecule at the gold surface. In fact, FTIRRAS data clearly show that strong adsorbed species form at low potentials (Figs. 11, 12). The presence of a second time constant in the case of TMTU can be assigned to the electroreduction process observed at such potentials (Fig. 1a, b), which, according to a previous data [15], would correspond to a partial reduction of the TMTU molecule, as it was revealed by the appearance of S-H IR bands in the –0.6 to –0.8 V range. Assuming a double-layer capacitance of ca. 80 μF cm^{-2}, a capacitance of ca. 166 μF cm^{-2} is obtained for the adsorbed layer. The high values of the charge transfer resistance in this potential range indicates that the electrosorption of TUs is a rather slow electrochemical process that can be written as [27, 34]

$$\mathrm{Au} + \mathrm{TUs(sol)} \leftrightharpoons \mathrm{AuTUs^{+}_{ads}} + e^{-} \qquad (6)$$

It is interesting to note that as the potential moves to less negative values, the charge transfer resistance increases markedly for the case of TU, about one order of magnitude, and the impedance response results in the appearance of an open semicircle. This indicates that adsorbed TU is very stable in this potential region.

When the electrode potential increases from ca. –0.25 V upwards, the polarisation curves show the appearance of a net anodic current that steadily increases with the potential. While for TU solution one observes a net current peak with shoulders on the ascending and descending sides of the peak, for TMTU solution one observes the presence of a rather limiting current region before the appearance of an

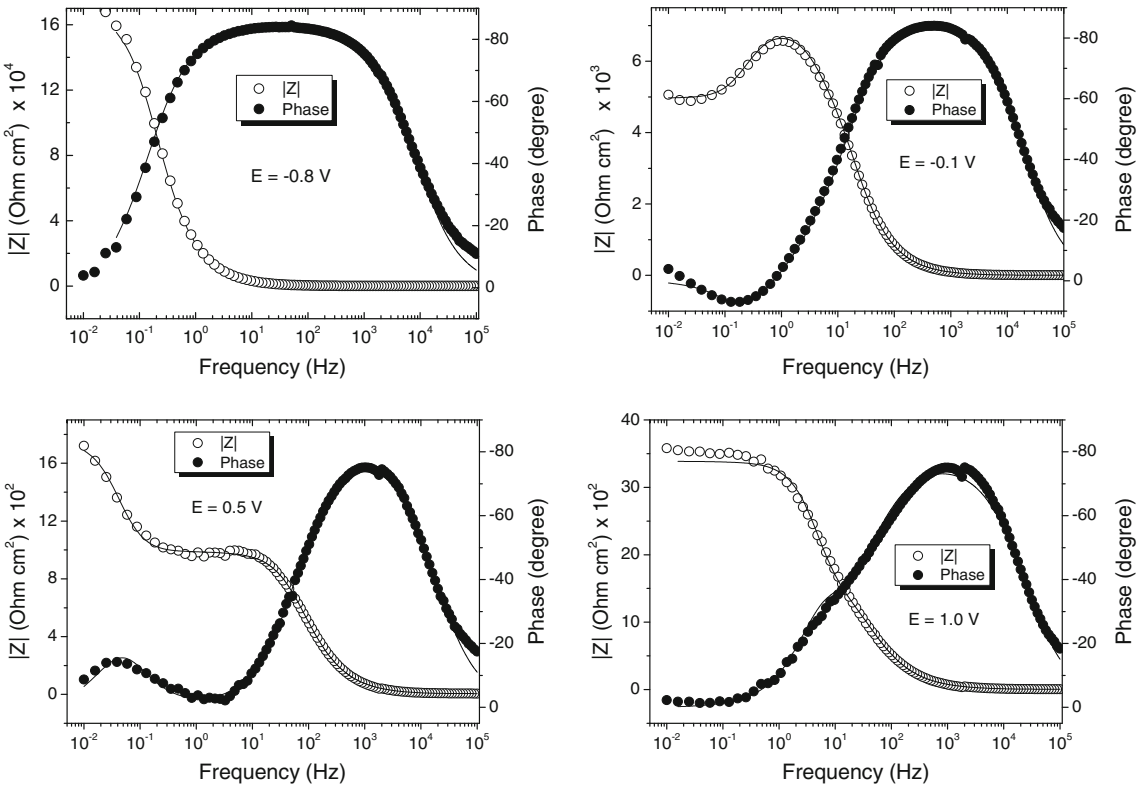

Fig. 14 Experimental and fitted Bode plots for gold RDE in aqueous 1 mM TU + 0.5 M sulphuric acid according to Eq. (3) (**a**, **b**) and Eq. (4) (**c**, **d**). The corresponding equivalent circuits are shown in Fig. 13 and parameters are assembled in Table 1

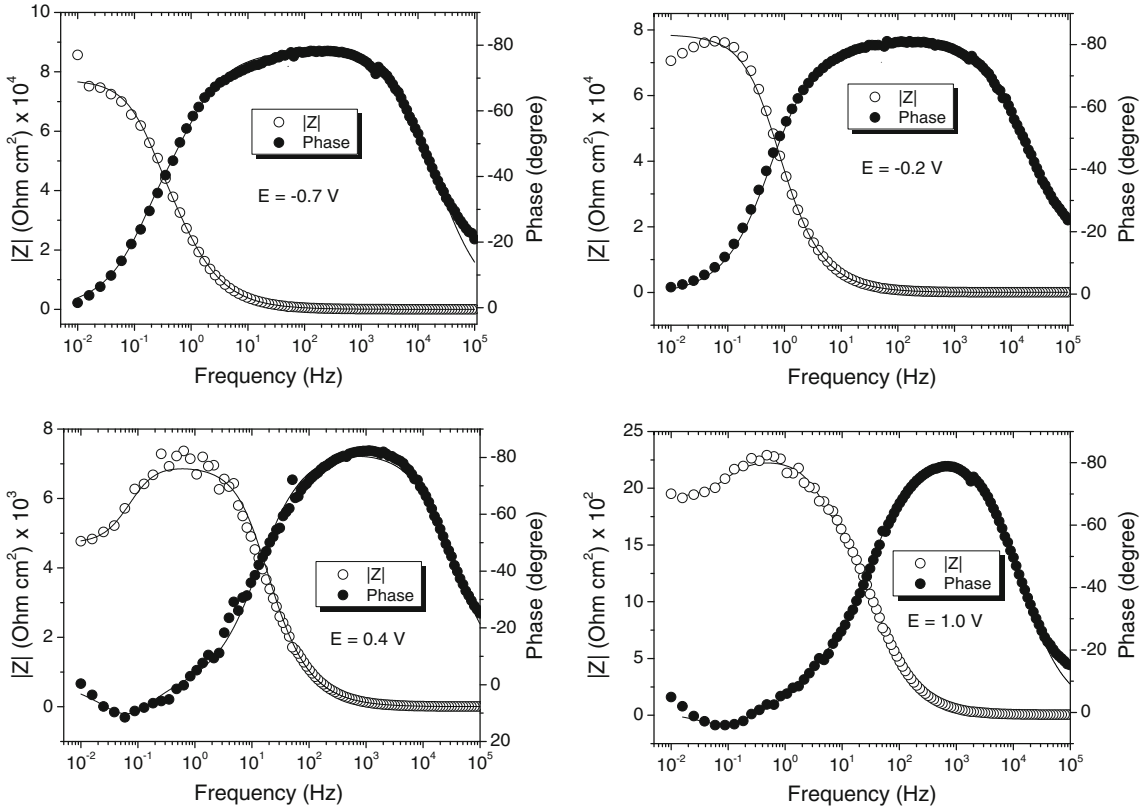

Fig. 15 Experimental and fitted Bode plots for gold RDE in aqueous 1 mM TMTU + 0.5 M sulphuric acid according to Eq. (3) (**a**, **b**) and Eq. (4) (**c**, **d**). The corresponding equivalent circuits are shown in Fig. 13 and parameters are assembled in Table 1

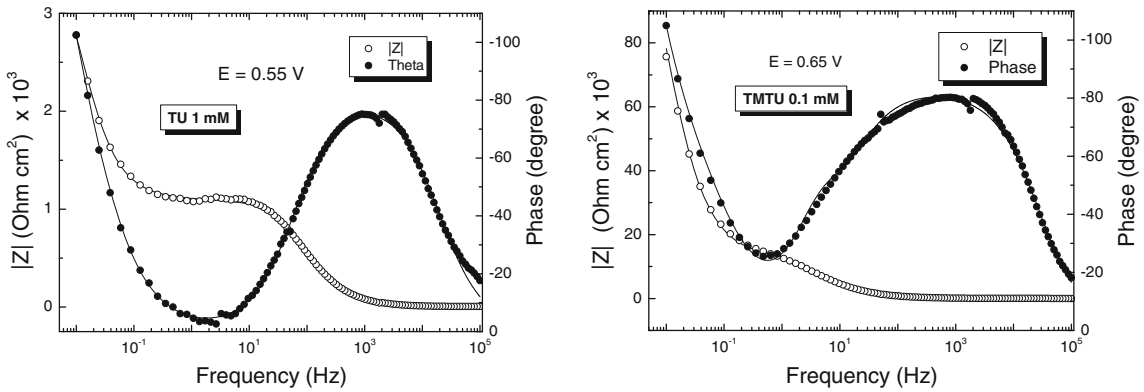

Fig. 16 Experimental and fitted Bode plots for gold RDE in aqueous 1 mM TU and 0.1 mM TMTU + 0.5 M sulphuric acid according to Eq. (5). The corresponding equivalent circuits are shown in Fig. 13 and parameters are assembled in Table 1

anodic current peak (Fig. 1). These features are independent of the additive concentrations used in this work. The anodic current appears at less positive potentials in the case of 1 mM TMTU solution, although for TU it reaches higher values (Fig. 1a). In this potential range the Nyquist plots consist of two capacitive contributions and an inductive loop at low frequencies. The appearance of the inductive contribution takes place concomitantly with an appreciable decrease in the charge transfer resistance. Inductive loops can be assigned to a relaxation process such as the desorption of TUs or the strong dissolution of the electrode. SEM images obtained for both additives show the formation of pits on the electrode surface, which is consistent with the appearance of inductive loops. The electrodissolution of gold in the presence of TUs can be interpreted through the following equation:

$$\mathrm{Au}(X)_{\mathrm{ad}} + X(\mathrm{aq}) \leftrightharpoons [\mathrm{Au}(X)_{\mathrm{n}}]^{+}(\mathrm{aq}) + \mathrm{e}^{-}, \qquad (7)$$

Table 1 Parameters resulting from experimental data fits shown in Figs. 14, 15 and 16

E/V	$R_S(\Omega\ cm^2)$	CPE ($\mu F\ cm^{-2}$)	α	$R_1(\Omega\ cm^2)$	$C_2(\mu F\ cm^{-2})$	$R_2(\Omega\ cm^2)$	$R_3(\Omega\ cm^2)$	$L(\Omega\ cm^2)$
	TU 1 mM							
−0.8	0.69	53	0.93	5×10^3				
−0.1	0.65	20	0.96	5,320	8×10^{-3}			258×10^3
0.5	0.68	35	0.92	118	47×10^{-3}			93
1.0	0.60	48	0.88	225	159			192
E/V	$R_s(\Omega\ cm^2)$	CPE ($\mu F\ cm^{-2}$)	α	$R_1(\Omega\ cm^2)$	$C_2(\mu F\ cm^{-2})$	$R_2(\Omega\ cm^2)$	$R_3(\Omega\ cm^2)$	$L(\Omega\ cm^2)$
	TMTU 1 mM							
−0.7	0.67	54	0.87	7,200	168	2,187		
−0.2	0.68	30	0.88	2	3.52	10,025		
0.4	0.70	19	0.92	7.93	0.019	579	278	591
1.0	0.62	38	0.93	179	587	60	40	68
E/V	$R_s(\Omega\ cm^2)$	CPE ($\mu F\ cm^{-2}$)	α	$R_1(\Omega\ cm^2)$	C_2 ($\mu F\ cm^{-2}$)	$R_2(\Omega\ cm^2)$	$CPE_2(\Omega\ cm^2)$	α	$R_4(\Omega\ cm^2)$
	TMTU 0.1 mM								
0.65	0.56	2.55×10^{-5}	0.94	765	7.58×10^{-7}	781	8×10^{-4}	0.78	−14.5
	TU 1 mM								
0.55	0.52	2.79×10^{-5}	0.86	0.66	7×10^{-6}	136	0.022	0.83	−532

where X represents either TU or TMTU, the value of n depending on the type of thiourea, i.e. 1 for TMTU [15, 27] and 2 for TU [21, 29].

Furthermore, the inductive loop appears concomitantly with a marked decrease in the value of the second time constant, i.e. the value of the capacitance and the resistance associated with this time constant decrease with E, as expected for the formation of adsorbed species on the electrode surface and the presence of a facilitated electron charge transfer. The real part of the interface impedance decreases one order of magnitude when the inductive contribution appears. This appears to be related to a strong decrease in the value of the first charge transfer resistance. The value of this resistance is significantly lower for TMTU with respect to TU, a fact that suggests that the electrodissolution of gold is greater in TMTU than in TU. This is consistent with the increased data scattering at low f for TMTU and agrees with data reporting a strong dissolution of gold in the presence of TMTU [15]. According to FTIRRAS [15, 32], the formation of soluble gold complexes is concomitant with the electro-oxidation of TUs producing the respective formamidinium disulphide, but the formation of the soluble complex can predominate over disulphide formation according to FTIRRAS and EQCM experiments for TU [21, 28, 31] and TMTU [34].

The second capacitive constant appearing in this potential region should then be related to the electro-oxidation of TUs according to

$$\mathrm{Au}(X)_{\mathrm{ad}} + X(\mathrm{aq}) \rightleftharpoons [X]_2^{2+} + 2\mathrm{e}^- + \mathrm{Au}. \quad (8)$$

As this reaction occurs concomitantly with the electrodissolution of gold, the corresponding time constants appear overlapped in the Nyquist plots.

As the potential moves towards ca. 0.55–0.6 V, the Nyquist plots show the appearance of a negative resistance which indicates a passivation of the electrode surface. This occurs when the electrode potential reach the values related to the initial stages of the oxide formation on gold [35]. Furthermore, for the case of TU, FTIRRAS showed the formation of NH_2CN [21, 32] in this potential range, and the appearance of this species should be accompanied by the formation of sulphur atoms on the gold surface [21], a fact that also agrees with the detection of an amorphous sulphide phase during the electro-oxidation of TU on gold by SERS measurements [18].

Once the passivation region is overcome, the Nyquist plots show once again the contribution of two capacitive constants and an inductive loop in the low-frequency range, being the inductive contribution more relevant in the case of TMTU, probably because gold dissolution is relatively more favoured by the presence of TMTU. In any case, FTIRRAS demonstrated the formation of soluble gold complex species for TU and TMTU in the potential region above 0.7 V [15, 21].

The decrease in the TUs concentration allows to diminish the contribution of the electrodissolution reaction,

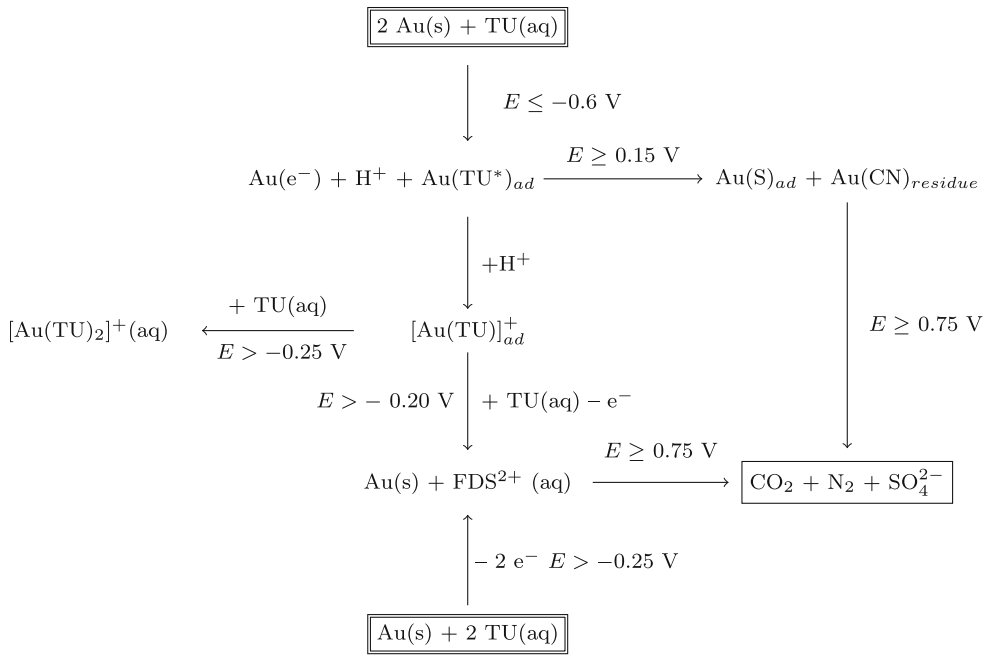

Fig. 17 Scheme of the electrochemical behaviour of TU and TMTU on gold in acid

particularly for the case of TMTU. For instance, the presence of a passivation process appears rather incipient in the case of 1 mM TMTU (Fig. 7c) but is clearly observed at 0.1 mM (Fig. 9b).

5 Conclusions

The investigation of the electrochemical behaviour of TU and TMTU on gold in acid by EIS complements the information reported in the literature from voltammetry, FTIRRAS, EQCM and SERS data. It shows the presence of a large charge transfer resistance and low capacity related to the formation of an adsorbed layer of TUs at low potentials. As the potential increases, the appearance of relaxation processes due to the electrodissolution of gold and the parallel contribution of a second electrochemical reaction related to the electro-oxidation of TUs is detected. The EIS experiments also allowed to detect the formation of a passive layer that diminishes the gold dissolution processes. This passivation region covers a potential window of about 0.15 V and beyond that the reactivation of the electrode surface takes place and both the second electro-oxidation stages of TUs, to produce carbon dioxide, sulphate ions and nitrogen species, and the electrodissolution of gold, via a soluble complex species, take place. The electrodissolution of gold increases with TUs concentration and from the comparison of the EIS behaviour of TU and TMTU, it appears that this process is enhanced for the case of TMTU.

A global overview of the electrochemical behaviour of TUs is summarized in the scheme of Fig. 17

Acknowledgments This work was financially supported by the Agencia Nacional de Promoción Científica y Tecnológica of Argentina (ANPCYT, PICT 2008-1902), the Consejo Nacional de Investigaciones Científicas y Técnicas (CONICET) and the Comisión de Investigaciones Científicas de la Provincia de Buenos Aires (CICPBA). AEB is member of CICPBA

References

1. Lawrence RW, Marchant P (1987) In: Salter RS, Wyslouzil DM, McDonald GW (eds) Gold metallurgy. Pergamon Press, New York
2. Chandra I, Jeffrey MI (2004) Hydrometallurgy 73:305
3. Yang X, Moats MS, Miller JD (2010) Electrochim Acta 55:3643
4. Li J, Miller JD (2002) Hydrometallurgy 63:215
5. Zhang H, Ritchie IM, Brooy SRL (2001) J Electrochem Soc 148:D146
6. Pesic B, Seal T (1990) Metall Trans 21B:419
7. Gaspar V, Mejerovich AS, Meretukov MA, Schmiedl J (1994) Hydrometallurgy 34:369
8. Tremblay L, Deschênes G, Ghali E, McMullen J, Lanouette M (1996) Int J Miner Process 48:225
9. Kai T, Hagiwara T, Haseba H, Takahashi T (1997) Ind Eng Chem Res 36:2757
10. Aguayo Salinas S, Encinas Romero MA, González I (1998) J Appl Electrochem 28:417
11. Chai L, Okido M, Wei W (1999) Hydrometallurgy 53:255
12. Porter LC R Acad Sci, Fackler JP, Costamagna J, Schmidt R (1992) Acta Cryst C48:1751
13. Piro OE, Castellano EE, Piatti RCV, Bolzán AE, Arvia AJ (2002) Acta Cryst C58:252

14. Bunge E, Port SN, Roelfs B, Meyer H, Baumgärtel H, Schiffrin DJ, Nichols RJ (1997) Langmuir 13:85
15. Bolzán AE, Iwasita T, Arvia AJ (2005) Electrochim Acta 51:1044
16. Groenewald T (1976) Hydrometallurgy 1:277
17. Schulze RG (1984) J Metals 36:62–66
18. Parker GK, Hope GA (2008) Miner Eng 21:489
19. Groenewald T (1975) J Appl Electrochem 5:71
20. Iwasita T (2002) Electrochim Acta 47:3663
21. Garcia G, Rodriguez JL, Lacconi GI, Pastor E (2004) Langmuir 20:8773
22. Hoffmann M, Edwards JO (1977) Inorg Chem 16:3333
23. Bierbach U, Barklage W, Saak W, Pohl S (1992) Z Naturforsch 47b:1593
24. Bolzán AE, Güida J, Piatti RCV, Arvia AJ, Piro OE, Sabino JR, Castellano EE (2007) J Mol Struct 271:131
25. Bunge E, Nichols RJ, Baumgärtel H, Meyer H (1995) Ber Bunsenges Phys Chem 99(10):1243
26. Bunge E, Nichols RJ, Roelfs B, Meyer H, Baumgärtel H (1996) Langmuir 12:3060
27. Port SN, Horswell SL, Raval R, Schiffrin DJ (1996) Langmuir 12:5934
28. Tian M, Conway BE (2004) J Appl Electrochem 34:533
29. Bolzán AE, Piatti RCV, Arvia AJ (2003) J Electroanal Chem 552:19
30. Iwasita T, Nart F (1995) In: Gerischer H, Tobias CW (eds) Advances in electrochemical science and engineering, vol 4. Wiley-VCH, Weinheim, p 123
31. Shevtsova O, Bek R, Zelinskii A, Vais A (2006) Russ J Electrochem 42:239
32. Bolzán AE, Iwasita T, Arvia AJ (2003) J Electroanal Chem 554(555):49
33. Reddy SJJ, Krishnan VN (1970) J Electroanal Chem 27:473
34. Larsen AG, Johannsen K, Gothelf KV (2004) J Colloid Interface Sci 279:158
35. Woods R (1976) In: Bard AJ (ed) Electroanalytical chemistry, vol 9, chap 1. Marcel Decker, New York, p 98